Vedran Mrzljak
Vladimir Medica
Ozren Bukovac

DOI: 10.21278/TOF.40203
ISSN 1333-1124
eISSN 1849-1391

SIMULATION OF A TWO-STROKE SLOW SPEED DIESEL ENGINE USING A QUASI-DIMENSIONAL MODEL

Summary

The paper describes a diesel engine quasi-dimensional numerical model, implemented in a previously developed 0D model. The presented model uses direct solution to the conservation equations set for cylinder pressure and zone temperatures without numerical iterations which are customary in these models. Numerical model validation was performed on a four-stroke diesel engine at four operating points. After successful validation, modifications were implemented in the numerical model allowing the simulation of a marine two-stroke diesel engine. It is important to emphasize that the simulation model logic remained unchanged. The only significant differences are the changes in the engine working processes and different calculation of the engine operating parameters which are characteristic of two-stroke engines. The results of the diesel engine simulations using the quasi-dimensional model were compared to the test-bed measurements of the two-stroke engine found in available literature. Good agreement between the measurements and the simulation results for the two-stroke engine has been obtained. The developed quasi-dimensional numerical model can accurately predict operating parameters of the four-stroke and the two-stroke diesel engine.

Key words: *quasi-dimensional (phenomenological) model; fuel spray; combustion; diesel engine; numerical simulation*

1. Introduction

Quasi-dimensional numerical models have been developed as a compromise between 0D and CFD models used for running internal combustion engine simulations. 0D numerical models assume a homogeneous gas mixture in the cylinder, so they cannot predict engine emissions [1], [2]. CFD models enable the most detailed simulations, but these simulations are time consuming and their final results are often unreliable due to the unknown initial flow field and turbulence intensity details.

Initial development of quasi-dimensional models had started with the idea of the cylinder space division into two zones - a fresh mixture zone and a zone of combustion products [3], [4]. This kind of models can give initial predictions of engine emissions, but the results are not very precise.

Quasi-dimensional progress occurs at the moment when the cylinder volume division is performed in the manner that during fuel injection spray packages (volumes) are created, which accompany each injected fuel spray, Fig. 1. Outside the fuel spray area there is a large remaining zone without fuel (zone without combustion) [5], [6], [7]. Fuel spray packages are spatial creations annular in shape, and in the spray core they have a form of a truncated cone. Fuel injectors can have a plurality of nozzles, so separate volumes are created for each of the fuel sprays. The basic numerical model assumption states that there are no exchanges of mass and energy between spray packages. The only allowed mass exchange is the air entrainment from the zone without combustion into spray packages [8] when the necessary conditions in each spray package are fulfilled.

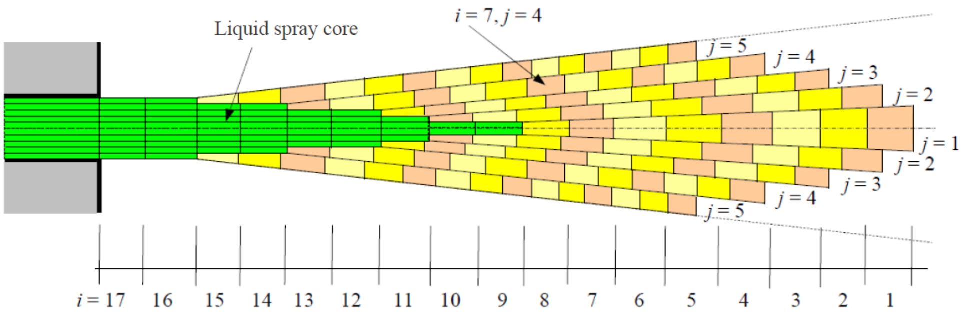

Fig. 1 Fuel spray divided into packages (volumes)

Many published scientific papers deal with the development and application of quasi-dimensional models. Papers [9] and [10] show the numerical analysis of quasi-dimensional models for a direct injection diesel engine simulation and provide an overview of engine emission calculations. Paper [11] presents the results of the quasi-dimensional model for diesel engine which uses a specific type of fuel - dimethyl ether. The authors in [12] show quasi-dimensional model results for diesel engines in severe operating conditions. Combustion simulations with quasi-dimensional models are shown in [13] and [14].

Recently, a number of quasi-dimensional model improvements have been introduced. One of the proposed improvements is the principle that parts of combustion products from spray packages are transferred into the zone without combustion. They are mixed with air and moved back into the packages [15], [16].

The quasi-dimensional model developed in [17] is applied in this paper and implemented in the existing 0D model [1] according to the model presented in [7]. The numerical model equations have been developed for a direct solution of pressure and temperature changes in the cylinder, without the necessity for time consuming numerical iterations.

2. Mathematical model

Starting from the mass, energy and momentum conservation equations, together with the gas state equation, a mathematical model for separate control volumes and for the whole cylinder content was developed. The mathematical expression (details are presented in [17]) gives the following differential equations of pressure and temperature changes in the engine cylinder:

$$A_\mathrm{i} = 1 + \frac{T_\mathrm{i}}{R_\mathrm{i}} \frac{\partial R_\mathrm{i}}{\partial T_\mathrm{i}}, \tag{1}$$

$$B_\mathrm{i} = 1 - \frac{p}{R_\mathrm{i}} \frac{\partial R_\mathrm{i}}{\partial p}, \tag{2}$$

$$C_{\mathrm{i}} = \left(\frac{\partial u_{\mathrm{i}}}{\partial p} \frac{p}{B_{\mathrm{i}}} \frac{A_{\mathrm{i}}}{T_{\mathrm{i}}} + \frac{\partial u_{\mathrm{i}}}{\partial T_{\mathrm{i}}} \right), \tag{3}$$

$$D_{\mathrm{i}} = \left(\frac{u_{\mathrm{i}}}{m_{\mathrm{i}}} + \frac{1}{m_{\mathrm{i}}} \frac{\partial u_{\mathrm{i}}}{\partial p} \frac{p}{B_{\mathrm{i}}} \right), \tag{4}$$

$$E_{\mathrm{i}} = \left(\frac{p}{m_{\mathrm{i}}} - \frac{1}{V_{\mathrm{i}}} \frac{\partial u_{\mathrm{i}}}{\partial p} \frac{p}{B_{\mathrm{i}}} \right), \tag{5}$$

$$F_{\mathrm{i}} = \left[\frac{1}{R_{\mathrm{i}}} \frac{\partial u_{\mathrm{i}}}{\partial p} \frac{p}{B_{\mathrm{i}}} G_{\mathrm{i}} + \left(\frac{\partial u_{\mathrm{i}}}{\partial \lambda_{\mathrm{i}}} \frac{\mathrm{d}\lambda_{\mathrm{i}}}{\mathrm{d}\varphi} + \frac{\partial u_{\mathrm{i}}}{\partial Y_{\mathrm{vap,i}}} \frac{\mathrm{d}Y_{\mathrm{vap,i}}}{\mathrm{d}\varphi} \right) \right], \tag{6}$$

$$G_{\mathrm{i}} = \left(\frac{\partial R_{\mathrm{i}}}{\partial \lambda_{\mathrm{i}}} \frac{\mathrm{d}\lambda_{\mathrm{i}}}{\mathrm{d}\varphi} + \frac{\partial R_{\mathrm{i}}}{\partial Y_{\mathrm{vap,i}}} \frac{\mathrm{d}Y_{\mathrm{vap,i}}}{\mathrm{d}\varphi} \right), \tag{7}$$

$$H_{\mathrm{i}} = \frac{C_{\mathrm{i}}}{\left(R_{\mathrm{i}} + T_{\mathrm{i}} \frac{\partial R_{\mathrm{i}}}{\partial T_{\mathrm{i}}} \right)}, \tag{8}$$

$$K_{1,\mathrm{i}} = \frac{B_{\mathrm{i}} u_{\mathrm{i}} T_{\mathrm{i}} \frac{\partial R_{\mathrm{i}}}{\partial T_{\mathrm{i}}} + p\, u_{\mathrm{i}} \left(\frac{p}{R_{\mathrm{i}}} - 1 \right) \frac{\partial R_{\mathrm{i}}}{\partial p}}{A_{\mathrm{i}} B_{\mathrm{i}} m_{\mathrm{i}} R_{\mathrm{i}}}, \tag{9}$$

$$K_{2,\mathrm{i}} = \frac{1}{m_{\mathrm{i}} R_{\mathrm{i}} A_{\mathrm{i}}} \frac{\partial u_{\mathrm{i}}}{\partial T_{\mathrm{i}}}, \tag{10}$$

$$K_{3,\mathrm{i}} = \frac{\left(u_{\mathrm{i}} + R_{\mathrm{i}} T_{\mathrm{i}} \right)}{m_{\mathrm{i}}} = \frac{h_{\mathrm{i}}}{m_{\mathrm{i}}}, \tag{11}$$

$$K_{4,\mathrm{i}} = \frac{\partial u_{\mathrm{i}}}{\partial T_{\mathrm{i}}} + R_{\mathrm{i}} A_{\mathrm{i}}, \tag{12}$$

$$S_1 = \sum_{\mathrm{i}} \left[\frac{\frac{1}{m_{\mathrm{i}}} \frac{\mathrm{d}Q_{\mathrm{i}}}{\mathrm{d}\varphi} - K_{1,\mathrm{i}} \frac{\mathrm{d}m_{\mathrm{i}}}{\mathrm{d}\varphi} + H_{\mathrm{i}} T_{\mathrm{i}} G_{\mathrm{i}} - F_{\mathrm{i}}}{K_{2,\mathrm{i}}} \right], \tag{13}$$

$$S_2 = \sum_{\mathrm{i}} \left(m_{\mathrm{i}} T_{\mathrm{i}} \frac{\partial R_{\mathrm{i}}}{\partial p} + \frac{\frac{E_{\mathrm{i}}}{p} \left(V_{\mathrm{i}} - m_{\mathrm{i}} T_{\mathrm{i}} \frac{\partial R_{\mathrm{i}}}{\partial p} \right)}{K_{2,\mathrm{i}}} \right), \tag{14}$$

$$\boxed{\frac{\mathrm{d}T_\mathrm{i}}{\mathrm{d}\varphi}=\frac{\dfrac{1}{m_\mathrm{i}}\dfrac{\mathrm{d}Q_\mathrm{i}}{\mathrm{d}\varphi}-K_{3,\mathrm{i}}\dfrac{\mathrm{d}m_\mathrm{i}}{\mathrm{d}\varphi}-F_\mathrm{i}}{K_{4,\mathrm{i}}}-\frac{\dfrac{E_\mathrm{i}}{p}\left[m_\mathrm{i}\,T_\mathrm{i}\,G_\mathrm{i}-\left(V_\mathrm{i}-m_\mathrm{i}\,T_\mathrm{i}\dfrac{\partial R_\mathrm{i}}{\partial p}\right)\dfrac{\mathrm{d}p}{\mathrm{d}\varphi}\right]}{K_{4,\mathrm{i}}},} \tag{15}$$

$$\boxed{\frac{\mathrm{d}p}{\mathrm{d}\varphi}=\frac{S_1-p\dfrac{\mathrm{d}V_\mathrm{c}}{\mathrm{d}\varphi}}{\left(V_\mathrm{c}-S_2\right)}.} \tag{16}$$

The variables A, B, C, D, E, F, G, H, K_1, K_2, K_3 and K_4 in equations (1) to (14) are substitutes for differential expressions, and parameters S_1, S_2 are the replacement for the sums that need to be inserted into the equation for the pressure change (16). The index i is the index for any observed control volume (for each package of each fuel spray as well as for the zone without combustion).

Regarding the fuel spray packages it should be noted that all of the equations are related to the thermodynamic (TD) volume of the package (volume of gases and vapours). The thermodynamic volume of the package is the geometric package volume reduced by the liquid fuel volume. The properties of the liquid fuel, which is also present in each fuel spray package, are monitored by separate mathematical models, independent of the presented one. The liquid fuel energy conservation equation was used to monitor the temperature, which is the basic parameter for the fuel evaporation calculation. Fuel vapour in this model is considered as an ideal gas in the gaseous mixture with other species.

According to Fig. 1, besides the indexes which are related to each package, (i = axial index, j = radial index), it was necessary to use an additional index k for each fuel spray when the fuel sprays are not identical one to another. In the case when fuel sprays are equal, only one spray is calculated, and the results are multiplied by the total number of sprays.

3. Engine data and measurement results of two-stroke diesel engine

Validation was performed on a high speed diesel engine with direct injection for the heavy freight vehicle drive MAN D 0826 LOH15. The validation results are presented in [17]. After successful validation, the numerical model was adjusted for the simulation of a two-stroke slow speed diesel engine. Numerical submodels for the slow speed diesel engine were taken from [18].

The quasi-dimensional model was used for the calculation of the high pressure part of the engine cycle, from the moment of suction ports closing until the moment of the exhaust valve opening. Because of that fact, the quasi-dimensional model was not affected by the exchange of the working fluid, so the rest of the two-stroke diesel engine model and its logic remained unchanged.

The accuracy check of the numerical model of the two-stroke engine was performed with test-bed measured data for a marine two-stroke diesel engine 6S50MC MAN B&W available in [19]. The basic engine performance and geometry characteristics are presented in Table 1.

The main operational data of the marine diesel engine are obtained by test-bed measurements. Table 2 presents the measured values for the selected engine steady operation at 25%, 50%, 75%, 93.5%, 100% and 110% of engine load. The engine was produced at the Shipyard Split under the MAN B&W license.

Table 1 Specifications of selected marine diesel engine 6S50MC MAN B&W

Data description	**Value**
Process type	two-stroke, direct injection
Number of cylinders	6 in line
Cylinder bore	500 mm
Stroke	1910 mm
Firing order	1-5-3-4-2-6
Maximum continuous rating (MCR)	8580 kW
Engine speed at MCR	127 min^{-1}
Maximum mean effective pressure	18 bar
Maximum combustion pressure	143 bar
Specific fuel consumption (with high efficiency turbocharger)	171 g/kWh, on 100% load
Compression ratio (obtained by calculation)	17.2
Crank mechanism ratio	0.436
Exhaust manifold volume	6.13 m^3
Inlet manifold volume (with intercooler)	7.179 m^3

Table 2 6S50MC MAN B&W measured data [19]

Engine load (regarding MCR)	**25%**	**50%**	**75%**	**93.5%**	**100%**	**110%**
Indicated power (kW)	2401	4406	6580	8170	8656	9499
Effective power (kW)	2142	4099	6160	7667	8182	9014
Engine speed (min^{-1})	76.5	96	110.4	118.5	121.4	125.2
Controller index	44.3	55.4	68.1	77.3	79.2	85.8
Compression pressure (bar)	46.2	70.3	97.5	117.6	123.7	137.8
Maximum combustion pressure (bar)	66.6	97.4	129.6	143.3	141.4	139.3
Mean indicated pressure (bar)	8.37	12.24	15.89	18.38	19.01	20.23
Fuel rack position (mm)	39.7	50.3	63.3	73	75	81.8
Intake manifold pressure (bar)	1.39	2.03	2.76	3.33	3.55	3.93
Intake manifold temperature (°C)	25	29	34	40	41	45
Exhaust manifold pressure (bar)	1.3	1.86	2.51	3.06	3.26	3.64
Temperature before the turbine (°C)	308	327	346	384	404	458
Turbocharger rotational speed (min^{-1})	7290	11360	13870	15360	15895	17110
Specific fuel consumption (g/(kW·h))	186.83	174.06	171.18	171.82	174.66	180.5

The examination was performed in the following environmental conditions:

- ambient temperature 30 °C,
- ambient pressure 1005 mbar,
- relative humidity 50%.

The engine was tested with diesel fuel D-2, whose properties are as follows:

- density 844.7 kg/m^3,
- kinematic viscosity 3.03 mm^2/s,
- sulphur content 0.45%,
- lower heating value 42.625 MJ/kg.

4. Numerical model results for diesel engine 6S50MC MAN B&W

The numerical model has been tested in the entire engine operating range. Agreement between the simulation and the measurement results is acceptable, with some minor deviations observed. The simulation results for eight working parameters of the simulated engine are presented, and finally an overview of the numerical simulation errors for each presented parameter is given.

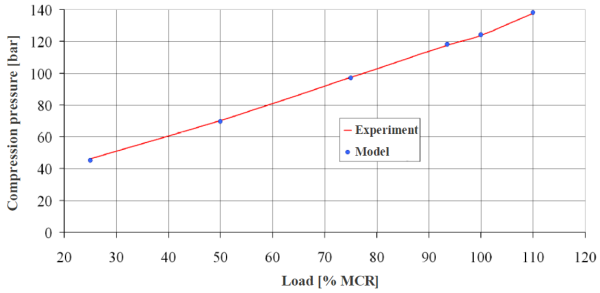

Fig. 2 Compression pressure for various engine loads

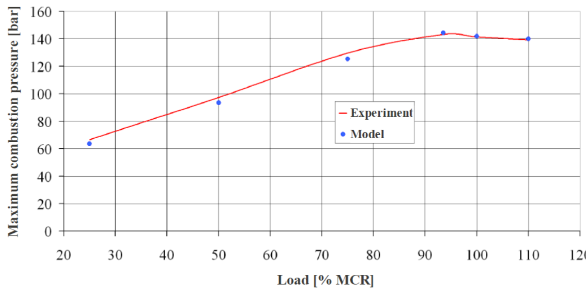

Fig. 3 Maximum combustion pressure for various engine loads

Fig. 2 presents the engine compression pressure changes, mainly due to the turbocharging conditions. For this working parameter, the simulation faithfully follows the measured results throughout the entire engine operating range. The largest simulation deviation is 2% at the lowest engine load (25% MCR).

Maximum combustion pressure changes can be seen in Fig. 3. Deviations between the simulation and the measurements are visible at lower engine loads (25%, 50% and 75% MCR). In this area, deviations are a result of the expected imprecision of the quasi-dimensional numerical model. At the moment, "allowed" errors for this working parameter in the CFD models are up to 3%. This quasi-dimensional numerical model gives the maximum error of 4.3% at the lowest engine load (25% MCR). For higher engine loads, the numerical model deviations are within 1% in comparison to the measurements.

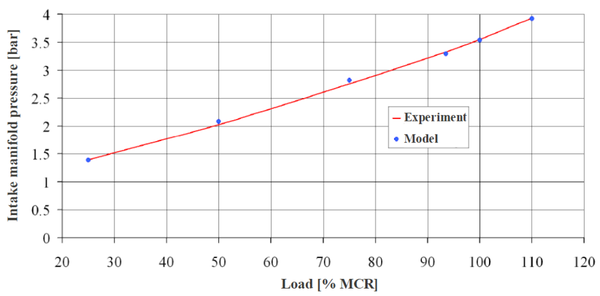

Fig. 4 Intake manifold pressure for various engine loads

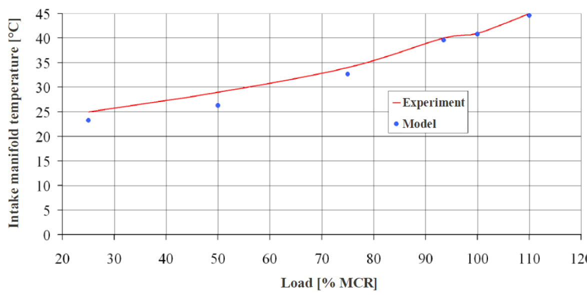

Fig. 5 Intake manifold temperature for various engine loads

For the observed engine some of the data related to the geometry of the intake and exhaust manifold were not available. Therefore, for the numerical simulations some of them were taken approximately from available data for similar two-stroke marine engines [20], [21].

Regardless of the incomplete input data, the simulation results and the measurement comparison of the intake manifold pressure, Fig. 4, are within acceptable deviations. The maximum deviation is 3% at the engine load of 50% MCR.

The impact of incomplete engine data is visible on the intake manifold temperature, Fig. 5. Greater deviations between the simulation and the measurements occur at lower engine loads. Maximum deviation of 9.5% is visible at the engine load of 50% MCR. At higher engine loads these deviations are within satisfactory values.

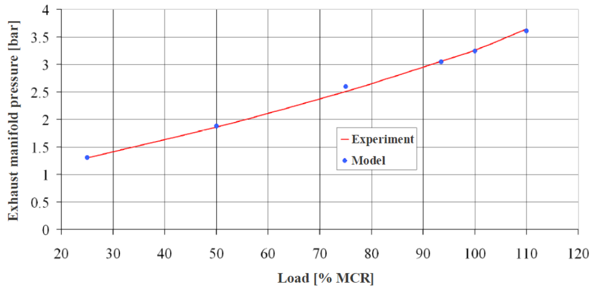

Fig. 6 Exhaust manifold pressure for various engine loads

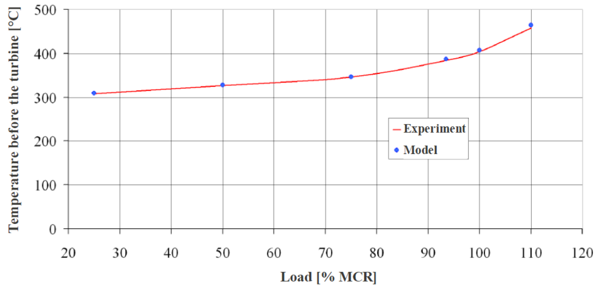

Fig. 7 Temperature before turbine for various engine loads

The exhaust manifold pressure, Fig. 6, despite a lack of accurate engine data, shows deviations similar to the intake manifold pressure, Fig. 4. The largest deviation for the exhaust manifold pressure is 3% at the engine load of 75% MCR.

Temperature before the turbine, Fig. 7, shows small simulation deviations compared to the measured values (deviations for the whole engine working area are within 2%).

From the presented results it can be concluded that the exhaust manifold geometry of the observed engine corresponds to the exhaust manifold geometry of similar engines. The intake manifold geometry of the observed engine is probably modified in relation to similar engines.

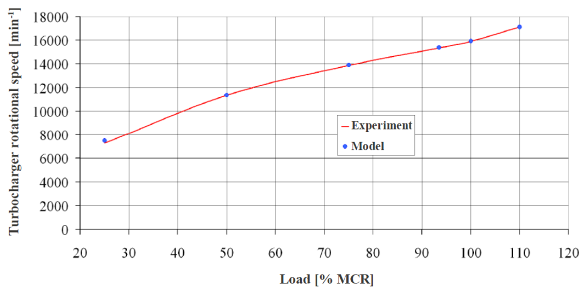

Fig. 8 Turbocharger rotational speed for various engine loads

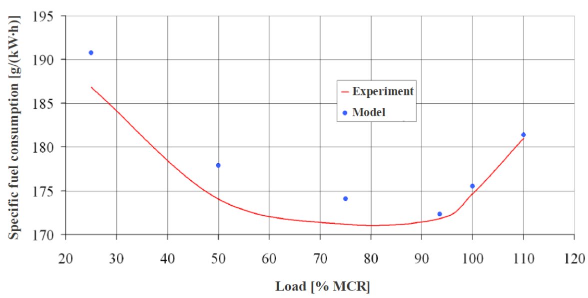

Fig. 9 Specific fuel consumption for various engine loads

The numerical model uses a separate submodel which calculates turbocharger operating parameters. The submodel is modelled in detail according to all available data for the examined engine turbocharger. Therefore, minimal simulation deviations are expected in comparison to the measured values for the turbocharger rotational speed, Fig. 8.

Specific fuel consumption is a very important operating parameter and has the greatest impact on system operating costs, in this case on the propulsion engine operating costs. The simulation results of this working parameter in relation to the measurements show acceptable deviations, less than 2.5% for the entire engine operating range, Fig. 9.

Simulation deviation changes in relation to the measured values for all monitored operating parameters are presented in Fig. 10 at all simulated engine loads. Fig. 10 shows that the deviations of the observed operating parameters, except for the intake manifold temperature, are within the range of ±4%.

From the presented results it can be concluded that the quasi-dimensional numerical model can predict operating parameters of the two-stroke slow speed diesel engine with significant reliability.

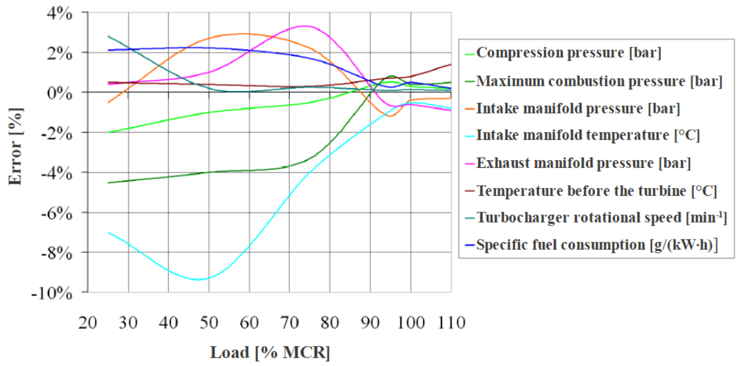

Fig. 10 Simulation errors for all presented working parameters of diesel engine 6S50MC MAN B&W

5. Conclusion

This paper presents a quasi-dimensional model developed for the numerical simulation of a two-stroke marine diesel engine. The quasi-dimensional model is implemented in an existing 0D model and is used as its integral part to simulate the high pressure engine process, i.e. from the moment of the intake ports closing until the moment of the exhaust valve opening.

The presented mathematical model, worked out in the equations, enables a direct calculation of the pressure and temperature changes in the cylinder, in order to avoid numerical iterations, which are customary in similar models. These equations accelerated the execution of the simulation model, so the simulation of one entire engine process in all cylinders together on a common desktop computer lasts about a minute.

The simulated working parameters for the low speed two-stroke diesel engine shows very good agreement with the test-bed measured values, except in the case of the results sensitive to the lack of data about the geometry of intake and exhaust that were not available. The developed numerical model has good accuracy and precision in the engine operating parameters prediction, within the expected error range for these models.

In addition to the presented operating parameters, the numerical model offers a number of other options, such as the calculation of engine emissions, excluding soot emission. For a detailed emission calculation, it is important to know the temperature distribution in the engine cylinder, and this model is able to calculate it as well. To obtain a complete overview of the engine emissions, this model must be upgraded with a numerical submodel for soot emission calculation, which is the goal of future research.

The developed quasi-dimensional model is a good compromise for engineers engaged in engine development. The simulation results are obtained quickly and it is possible to analyze the impact of design or certain parameters changes on the engine characteristics.

Nomenclature

λ	air excess ratio [-]
h	specific enthalpy [J/kg]
m	mass [kg]
p	pressure [Pa]
Q	heat amount [J]
R	gas constant [J/kg·K]
T	temperature [K]
u	specific internal energy [J/kg]
V	volume [m^3]
Y_{vap}	fuel vapour mass fraction [-]
c	cylinder
TD	thermodynamical (volume)

REFERENCES

[1] Medica, V.: Simulation of turbocharged diesel engine driving electrical generator under dynamic working conditions, Doctoral Thesis, University of Rijeka, Rijeka, 1988.

[2] Engl, G.: The modeling and numerical simulation of gas flow networks, Numerische Mathematik 72, 349-366, 1996. DOI: 10.1007/s002110050173

[3] Ishida, M., Chen, Z. L., Ueki, H., Sakaguchi, D.: Combustion Analysis by Two-Zone Model in a DI Diesel Engine, International Symposium COMODIA 94, 1994.

[4] Rakopoulos, C. D., Rakopoulos, D. C., Giakoumis, E. G., Kyritsis, D. C.: Validation and sensitivity analysis of a two zone Diesel engine model for combustion and emissions prediction, Energy Conversion and Management 45, p. 1471-1495, 2004. DOI: 10.1016/j.enconman.2003.09.012

[5] Yoshizaki, T., Nishida, K., Hiroyasu, H.: Approach to Low Nox and Smoke Emission Engines by Using Phenomenological Simulation, SAE Paper 930612, 1993.

[6] Salem, H., El-Bahnasy, S. H., Elbaz, M.: Prediction of the effect of injection parameters on NOx emission and burning quality in the direct injection diesel engine using a modified multizone model, IMechE, D01797, Vol. 212, Part D, 1998.

[7] Hiroyasu, T., Miki, M., Kamiura, J., Watanabe, S., Hiroyasu, H.: Multi-Objective Optimization of Diesel Engine Emissions and Fuel Economy using Genetic Algorithms and Phenomenological Model, SAE Technical Paper 2002-01-2778, 2002.

[8] Hiroyasu, H., Arai, M.: Structures of Fuel Sprays in Diesel Engines, SAE Paper 900475, 1990.

[9] Liu, Y., Midkiff, K. C., Bell, S. R.: Development of a multizone model for direct injection diesel combustion, IMechE, JER02601, Vol. 5, No. 1, 2004.

[10] Jung, D., Assanis, D. N.: Modeling of direct injection diesel engine emissions for a quasi-dimensional multi-zone spray model, International Journal of Automotive Technology, Vol. 5, No. 3, pp. 165-172, 2004.

[11] Meng, X., Jiang, Z., Wang, X., Jiang, D.: Quasi-dimensional multizone combustion model for direct injection engines fuelled with dimethyl ether, IMechE, D01403, Vol. 218, PartD, 2004.

[12] Tauzia, X., Maiboom, A., Chesse, P., Thouvenel, N.: A new phenomenological heat release model for thermodynamical simulation of modern turbocharged heavy duty Diesel engines, Applied Thermal Engineering 26, pp. 1851-1857, 2006. DOI: 10.1016/j.applthermaleng.2006.02.009

[13] Rakopoulos, C. D., Antonopoulos, K. A., Rakopoulos, D. C.: Multi-zone modeling of Diesel engine fuel spray development with vegetable oil, bio-diesel or Diesel fuels, Energy Conversion and Management 47, 1550-1573, 2006. DOI: 10.1016/j.enconman.2005.08.005

[14] Rakopoulos, C. D., Antonopoulos, K. A., Rakopoulos, D. C.: Development and application of multi-zone model for combustion and pollutants formation in direct injection diesel engine running with vegetable oil or its bio-diesel, Energy Conversion and Management, 2007. DOI: 10.1016/j.enconman.2007.01.026

[15] Poetsch, C., Ofner, H., Schutting, E.: Assessment of a Multi Zone Combustion Model for Analysis and Prediction of CI Engine Combustion and Emissions, SAE International, 2011-01-1439, 2011.

[16] Poetsch, C., Ofner, H., Cartellieri, W.: Analysis of Thermodynamic Characteristics of Diesel Engine Emission Control Strategies Using a Multi-Zone Combustion Model, SAE International, 2012-01-3340, 2012.

[17] Mrzljak, V.: Quasi-dimensional model for numerical simulations of marine two-stroke diesel engine, Doctoral Thesis, University of Rijeka, Rijeka, 2015.

[18] Mrakovčić, T.: Design and control of marine propulsion plant using numerical simulation, Doctoral Thesis, University of Rijeka, Rijeka, 2003.

[19] Račić, N.: Simulation of performance of the ship propulsion system with slow speed diesel engine in aggrivated conditions, Doctoral Thesis, University of Rijeka, Rijeka, 2008.

[20] http://www.wartsila.com/ (last visited: 02.12.15.)

[21] http://marine.man.eu/ (last visited: 02.12.15.)

Submitted: 14.12.2015

Accepted: 10.5.2016

dr. sc. Vedran Mrzljak
vedran.mrzljak@riteh.hr
prof. dr. sc. Vladmir Medica
dr. sc. Ozren Bukovac
Faculty of Engineering, University of Rijeka
Vukovarska 58
51000 Rijeka